

Earlier spring snowmelt in northern Alaska as an indicator of climate change

Robert S. Stone¹

Division of Cryospheric and Polar Processes, Cooperative Institute for Research in Environmental Sciences, University of Colorado, Boulder, Colorado, USA

Ellsworth G. Dutton, Joyce M. Harris, and David Longenecker²

Climate Monitoring and Diagnostics Laboratory, National Oceanic and Atmospheric Administration, Boulder, Colorado, USA

Received 20 December 2000; revised 11 June 2001; accepted 6 September 2001; published 22 May 2002.

[1] Predictions of global circulation models (GCMs) that account for increasing concentrations of greenhouse gases and aerosols in the atmosphere show that warming in the Arctic will be amplified in response to the melting of sea ice and snow cover. There is now conclusive evidence that much of the Arctic has warmed in recent decades. Northern Alaska is one region where significant warming has occurred, especially during winter and spring. We investigate how the changing climate of northern Alaska has influenced the annual cycle of snow cover there and in turn, how changes in snow cover perturb the region's surface radiation budget and temperature regime. The focus is on Barrow, Alaska, for which comprehensive data sets exist. A review of earlier studies that documented a trend toward an earlier disappearance of snow in spring is given. Detection and monitoring activities at Barrow are described, and records of snow disappearance from other sites in the Alaskan Arctic are compared. Correlated variations and trends in the date of final snowmelt (melt date) are found by examining several independent time series. Since the mid-1960s the melt date in northern Alaska has advanced by ~ 8 days. The advance appears to be a consequence of decreased snowfall in winter, followed by warmer spring conditions. These changes in snowfall and temperature are attributed to variations in regional circulation patterns. In recent decades, there has been a higher frequency of northerly airflow during winter that tends to diminish snowfall over northern Alaska. During spring, however, intrusions of warm moist air from the North Pacific have become more common, and these tend to accelerate the ablation of snow on the North Slope of Alaska. One result of an earlier melt date is an increase in the net surface radiation budget. At Barrow, net radiative forcing can exceed 150 W m^{-2} on a daily basis immediately following the last day of snowmelt, and as a result of an 8-day advance in this event, we estimate an increase of $\sim 2 \text{ W m}^{-2}$ on an annual basis. Our results are in general agreement with earlier analyses suggesting that reductions in snow cover over a large portion of the Arctic on an annual basis have contributed to a warming of the Northern Hemisphere (NH). In addition, the terrestrial ecosystems of the region are very sensitive to snow cover variations. There is growing concern that these perturbations are anthropogenically forced and adapting to these environmental changes will have significant social and economic consequences. While observed decreases in NH snow cover are in broad agreement with GCM simulations, our analyses suggest that internal (or natural) shifts in circulation patterns underlie the observed variations. Continued monitoring and further study is needed to determine whether the earlier disappearance of snow cover in spring in northern Alaska is an indicator of greenhouse-forced global warming or is a manifestation of a more natural, long-term cycle of climate change. *INDEX TERMS:* 3300 Meteorology and Atmospheric Dynamics; 3309 Meteorology and Atmospheric Dynamics: Climatology (1620); 3349 Meteorology and Atmospheric Dynamics: Polar meteorology; 3359 Meteorology and Atmospheric Dynamics: Radiative processes; *KEYWORDS:* arctic, snowmelt, temperature-albedo feedback, radiation budget

¹Also at Climate Monitoring and Diagnostics Laboratory, National Oceanic and Atmospheric Administration, Boulder, Colorado, USA.

²Also at Cooperative Institute for Research in Environmental Sciences, University of Colorado, Boulder, Colorado, USA.

1. Introduction

[2] Climate simulations that account for increasing concentrations of greenhouse gases show that global warming will reduce Arctic snow and ice cover, resulting in a decrease in surface albedo [Houghton *et al.*, 1996]. Lower albedo will increase solar absorption by the surface and promote further warming. This temperature-albedo feedback [e.g., Curry *et al.*, 1995] is one reason why

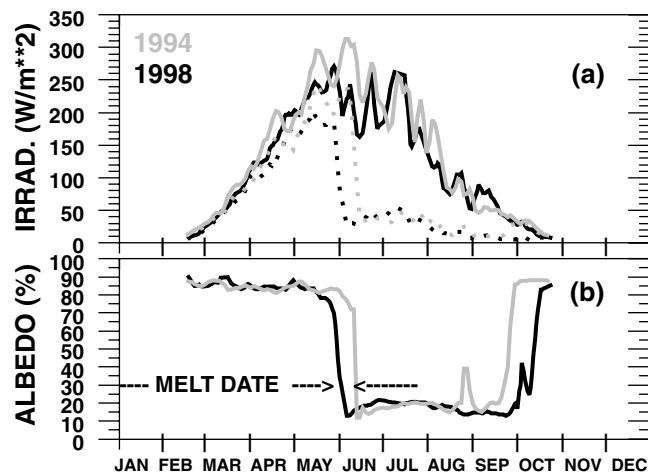


Figure 1. Seasonal cycles of (a) downwelling (S_D , solid curves) and upwelling (S_U , dashed curves) solar irradiance at NOAA/Climate Monitoring and Diagnostics Laboratory Barrow Observatory (CMDL-BRW), representing late (1994, shaded curves) and early (1998, black curves) spring melt seasons, and (b) derived albedos ($\alpha = S_U/S_D$) for the same 2 years. A 30% albedo threshold

observers look to the Arctic for early indications of global warming. Much of the Arctic has already warmed significantly [Serreze et al., 2000]. Decreases in Northern Hemisphere (NH) snow cover have been documented [Brown and Braaten, 1998; Groisman et al., 1994; Robinson et al., 1993]. Sea ice has diminished [Vinnikov et al., 1999; Maslanik et al., 1999, 1996], and there is evidence that a significant thinning of Arctic sea ice has occurred since the 1960s [Rothrock et al., 1999]. Vinnikov et al. [1999] claim that the decrease in sea ice extent is outside the range of natural variability, suggesting that global warming due to anthropogenic causes underlies the trend. In turn, changing climatic conditions in the high northern latitudes have influenced biogeochemical cycles. One consequence of an earlier disappearance of snow cover in spring is the lengthening of the active growing season [Myneni et al., 1997]. An early and longer growing season tends to increase the amplitude of the annual cycle of CO_2 [Keeling et al., 1996], and there is also evidence that the Arctic tundra is becoming a net source of CO_2 [Oechel et al., 1995]. Other studies show that Arctic permafrost is thawing [Osterkamp and Romanovsky, 1999]. When permafrost thaws, tundra wetlands and thermokarst lakes expand in area, releasing greater amounts of methane into the atmosphere. Zimov et al. [1997] suggest that methane released from such areas has enhanced the annual cycle of methane at high latitudes in recent years. In turn, the factors mentioned above impact plant and animal habitats and thus impact the productivity of fishing and hunting grounds that indigenous people depend on. There is a growing concern that an amplification of global warming in the Arctic will have a major effect on the ecosystems there.

[3] Despite the diverse and convincing observational evidence that the Arctic environment is changing, it remains unclear whether these changes are anthropogenically forced or result from more natural variations of the climate system. Because any long-term change in the distribution of snow will perturb the energy balance of the Arctic and in turn, perturb its sensitive terrestrial ecosystems, a better understanding of what controls the seasonal accumulation and ablation of snow is needed.

[4] In this paper we investigate some of the physical processes that influence the annual cycle of snow cover on the North Slope of Alaska, document a recent trend toward an earlier disappearance of snow in spring, and quantify the radiative effects of this earlier

disappearance of snow cover. The analyses are empirical and draw on correlative evidence from carefully assimilated data sets. Sections 2 and 3 provide an overview and update of time series analyses of the date of snow disappearance in the vicinity of Barrow, Alaska, with descriptions of detection and monitoring activities. Supporting evidence from several other North Slope sites that the spring melt season has advanced in recent decades is also given in section 3. Sections 4 and 5 identify some key factors that influence the annual snow cycle of the Alaskan Arctic and describe some of the physical processes that affect snow ablation rates. Section 6 presents an analysis of airflow trajectories in conjunction with synoptic maps that reveal underlying patterns of circulation that affect the precipitation and temperature regimes of northern Alaska. In section 7 the radiative impact of an earlier disappearance of snow cover in spring is discussed, and evidence of a temperature-albedo feedback is presented. Conclusions and final remarks are given in section 8.

2. A History of Analyses of the Barrow, Alaska, Snowmelt Date

[5] On the basis of snow depth measurements, Foster [1989] found that the date in spring when the tundra became snow-free at the Barrow National Weather Service (NWS) had occurred progressively earlier since the 1940s. Dutton and Endres [1991] suggested that the trend was attributable to local effects related to rapid development in the village of Barrow that is adjacent to the NWS station. They used radiometric data (1986–1990) from the National Oceanic and Atmospheric Administration (NOAA) Climate Monitoring and Diagnostics Laboratory (CMDL) Barrow Observatory (BRW), combined with the earlier radiometric observations of Maykut and Church [1973] and Weller and Holmgren [1974], to show that the NWS trend was not representative of the open tundra nearby. BRW (71.3°N, 156.6°W; elevation 8 m above sea level (asl)) is located 8 km upwind of town where the influence of development is minimal. In a follow-on study, Foster et al. [1992] analyzed NOAA satellite imagery to determine the date of snow disappearance at four Arctic locations. The study areas consisted of narrow strips of land, 10° longitude in width between 66°N and 70°N latitude. Representative sites were chosen in Alaska, Canada, Siberia, and Scandinavia to give a panarctic perspective of the timing of the final disappearance of snow cover. With the exception of the Siberian record, the analyses indicated a tendency toward an earlier snowmelt in spring. Ancillary in situ data were presented as validation of the satellite observations. With an additional 10 years of data now available, we update the Barrow time series and analyze ancillary data to arrive at an explanation of why snow appears to be melting earlier in spring in that region of the Arctic.

3. Detection and Monitoring of Snow Disappearance in Northern Alaska

3.1. Determination and Trend Analyses of Melt Dates in the Vicinity of Barrow

[6] Figure 1 illustrates how the disappearance of snow at BRW is determined from surface albedo (α) derived from measurements of upwelling (S_U) and downwelling (S_D) solar irradiance ($\alpha = S_U/S_D$). A daily average threshold of $\alpha = 0.30$ (30%) is used to determine the final day of melt there, i.e., when the snow cover essentially disappears. During the final week, α falls rapidly from ≥ 0.75 to $\sim 0.17 \pm 0.03$. The choice of 30% is based on historical considerations that are described fully by Dutton and Endres [1991]. Although at 30% albedo some snow remains on the ground, this is consistent with visual observations used in the earlier study of Foster [1989], who determined melt date as the day [Foster, 1989, p. 63] “when the stable, seasonal snow cover finally disappears in

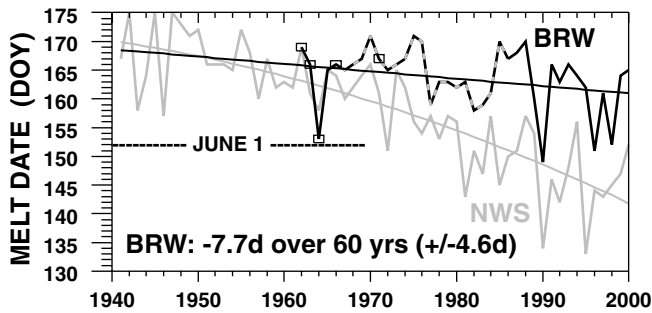


Figure 2. Time series of melt dates at the Barrow National Weather Service (NWS, shaded curves) compared with a BRW record comprised of historical (squares) and NOAA/CMDL-BRW radiometric (solid, black curve) observations and proxy estimates determined from temperature records (dashed curve). The BRW time series, merged with the 1941–1961 NWS record, was fitted linearly to yield the trend indicated in the legend, significant at the 95% confidence level.

the spring.” This was quantified as being [Foster, 1989, p. 64] “when 1 inch of snow (2.5 cm) can no longer be measured . . .” In this paper we define “melt date” on this historical basis, recognizing that the complete disappearance of snow can be greatly delayed if larger snowdrifts persist for many days after the tundra is essentially snow-free.

[7] Figure 2 compares time series of NWS and BRW melt dates as defined above. On the basis of site visits during recent melt seasons and an examination of aerial photographs and growth statistics, we conclude that the divergence of the two time series is due to progressive development near the NWS site, beginning around the mid-1960s. The contamination has resulted primarily from (1) mechanical ablation by snowmobiles and foot traffic, (2) decreasing snow albedo due to road dust and exhaust emissions, and (3) a possible reduction in snow accumulation locally caused by newer construction upwind of the observing site. These human influences are difficult to quantify, so we are unable to detect a natural climate signal in the NWS record. Instead, we analyze the BRW record, shown in Figure 2 as a merged time series of NWS observations (1941–1961), and albedo-determined melt dates derived from the recent BRW (1987–2000) and earlier radiometric observations of *Maykut and Church* [1973] and *Weller and Holmgren* [1974] (1962–1965 and 1971). Data gaps are filled using proxy observations, which are estimates made from the examination of time series of daily mean air temperature that show a signature related to the final phase of the melting process. At BRW the melt date occurs after ~8 days of average temperature near freezing ($\pm 1^{\circ}\text{C}$) followed by an abrupt warming as albedo decreases, solar absorption increases, and the near-surface air warms in response. In over 85% of cases, by identifying these features, we can determine the day when the snow cover disappears to within 2.5 days of dates determined radiometrically. A similar approach was used by *Zhang et al.* [1997] to determine the disappearance of snow in spring at three sites in the lower Kuparuk River basin. Sharp increases in the daily amplitude of ground temperatures were found to coincide with the final day of snowmelt.

[8] A linear fit of the BRW time series of melt date (Figure 2) shows an advance of 7.7 days (± 4.6) over 60 years at the 95% confidence level. The NWS time series was fitted with a quadratic because of the increasing downward tendency indicated. The NWS record shows an advance in the melt date of ~1 month over the 60-year period. Unfortunately, this (in-town) record can no longer be used to assess climate change because of the urbanization effects mentioned above.

3.2. Ancillary Records of the Date of Final Snowmelt in Northern Alaska

[9] Figure 3a shows time series of the day of year (DOY) when the snow cover disappears at four other North Slope sites shown on the accompanying map (Figure 3b). Two proxy observations (upper two curves) that are related to the disappearance of the snow cover are also shown. Each time series is evaluated for a trend and is cross-correlated with its overlap with the BRW record of melt date. Correlation coefficients (r) are given in brackets, labeled by location and color coded. Although yearly data were analyzed, only 5-year smoothed data are presented in Figure 3 for the sake of clarity. The average standard deviation (SD) of the linear regressions, weighted by the number of years in respective time series, is 6.3 days. Therefore, 95% (2 SDs) of all observed and proxy melt dates occur within a 25-day range centered on those respective trend lines.

[10] In Figure 3a the Sagwon (69°N , 148.8°W ; elevation 351 m asl) and Franklin Bluffs (69.9°N , 148.1°W ; elevation 76 m asl) melt dates were determined using the 0.30 albedo threshold (e.g., Figure 1). Both sites are within the Kuparuk River Watershed [Kane et al., 2000], located southeast of Barrow. Barter Island (70.1°N , 143.6°W ; elevation 15 m asl) was another NWS station where, until 1987, the date of snow disappearance was determined from snow depth measurements using a trace, or <1-inch snow depth as the criteria [e.g., Foster, 1989]. The series labeled satellite was derived from visible satellite images of a strip of tundra ~150 km south of BRW. Although satellite observations were made beginning in 1976 [Foster et al., 1992], we discovered that prior to 1982 the

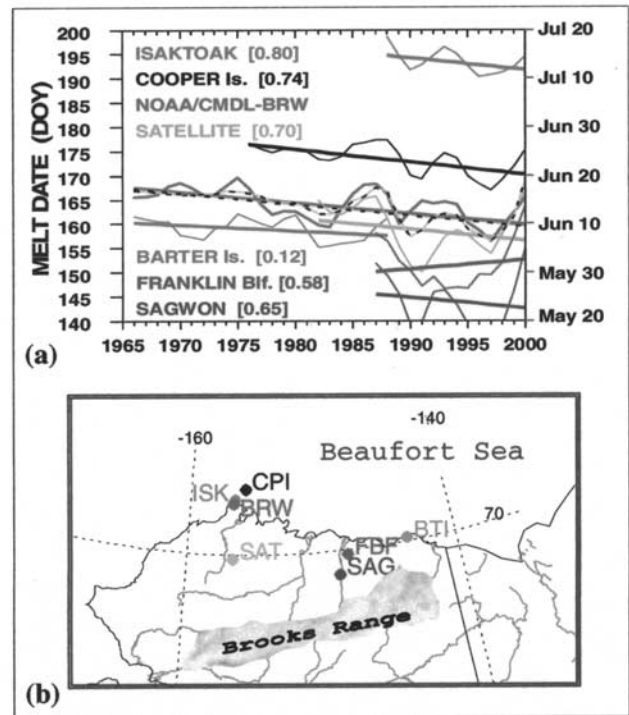


Figure 3. Analyses of six independent time series of melt dates compared with the 1966–2000 BRW record (from Figure 2). The 5-year smoothed time series and linear fits are shown. Each is correlated with the NOAA/CMDL-BRW record with coefficients indicated for each of the sites described in the text. The dashed-curve analysis (unlabeled) is for an ensemble average of the 142 station-years, normalized to the BRW timeframe. (b) Map of Alaska’s North Slope showing the location of sites making up the ensemble. Details of data and site descriptions are given in the text. See color version of this figure at back of this issue.

satellite-derived melt dates showed significant late biases when compared with the other records that, in recent years, are well correlated with the satellite observations. It is likely that the poorer temporal resolution of analyses, made only weekly in the early years, compounded by the presence of clouds, led to these delayed determinations of snow disappearance. For instance, if clouds obscured the sample location on a particular day of analysis but the tundra below was already snow-free, at least a week's delay in assigning a date of snow disappearance would result from using a weekly analysis frequency. The quality of the record has improved also because in recent years, analysts have had the benefit of multispectral radiance data to better distinguish clouds from snow (J. Foster, NASA-GSFC, personal communication, 2000). Inclusion of the 1976–1981 satellite data yields a linear trend that has twice the slope of the one shown in Figure 3a. Therefore we base the current satellite analysis only on the 1982–2000 period that appears to have the greatest validity. The high degree of correlation between the satellite and in situ observations of snow disappearance over the last 2 decades is very encouraging because remote sensing offers the only viable means to monitor snow cover spatially and temporally on an Arctic-wide basis. Every effort to exploit multispectral satellite data for this purpose should be made, using representative surface observations to validate and improve retrieval algorithms. Zhang *et al.* [2000] have made significant strides in this regard. Using albedo measurements from several tundra locations in combination with 1.25-km images from Advanced Very High Resolution Radiometers (AVHRR) onboard polar orbiting satellites, they were able to produce maps of Alaska's North Slope showing the pattern of surface albedo. A time history of such data can be used to observe the progression of the disappearance of snow over the course of a season using daily analyses. Multiyear analyses of this type on an Arctic-wide scale would be extremely valuable for assessing trends of snow cover and its spatial variability.

[11] The upper two curves in Figure 3a are proxy records. Cooper Island (71.7°N, 155.7°W; elevation 3 m) is a time series of dates when a species of Arctic seabird, the Black Guillemot, first lays eggs. Each year, Black Guillemots breed on the island, but not until the snow completely melts can they access nest cavities. The timing of the final melt is a crucial factor that affects the birds' breeding chronology and success rate because the species requires a snow-free cavity for at least 80 days, and the snow-free period in the vicinity of Barrow frequently was <80 days before the 1970s [Divoky, 1998]. Since the mid-1970s, Divoky has been going to the island during the final period of snowmelt to obtain information on their breeding chronology. The birds have an uncanny sense of when the snow disappears. Because ovulation cannot occur until females have access to the cavities, the appearance of the "first egg" is an excellent proxy indicator of snow disappearance on Cooper Island. The first egg in the colony appears ~2 weeks after nests are occupied.

[12] Isaktoak is a time series of dates when the Isaktoak Lagoon, located within the village of Barrow, becomes ice-free (C. George, Barrow Wildlife Division, private communication, 2000). Since 1988, George has kept an accurate record of the "ice out" date that he defines as the complete disappearance of ice on the lagoon. Despite a full month delay in the date of ice out on the lagoon, this proxy record also correlates well with the BRW melt date time series, suggesting that the timing of final snowmelt and ice melt are influenced by similar climatic factors. One important factor is the amount of snow that falls during winter. Because snow is an excellent insulator, the onset of ice melt is probably delayed until the ablation of overlying snow is nearly complete. This is true for ice on tundra lakes or for sea ice. Following a season of abnormally high snowfall in the region, the melting of ice may be delayed. If less snow accumulates during winter, however, and ablation rates are high during spring, the onset of ice melt can occur early, resulting in diminished sea ice

concentrations and extent. This is currently under investigation. Preliminary results indicate a significant positive correlation between the timing of the onset of sea ice melt in the Beaufort/Chukchi Sea region and the melt date at BRW (R. Stone and S. Drobot, unpublished data, 2001).

[13] The dashed curves in Figure 3a represent an ensemble average analysis of all observations normalized to the timing of the BRW melt date trend line. A linear fit of this 142 station-year record shows an advance in the spring melt of 8.0 days over 35 years ± 4.0 (at a confidence level of 95%), suggestive of a regional trend. However, the correlated variations of time series shown in Figure 3a are more indicative of climatic shifts or cycles than of a monotonic change. Variability appears to have increased since the mid-1980s, and the most recent years, 1999 and 2000, show a distinct upturn at all sites, most likely in response to a recent shift in the region's climate. The 2001 melt date (not shown) was again relatively late, occurring on DOY 162. This upturn affects the statistical analysis of the shortest records quite markedly. For Franklin Bluffs this is manifested as a reversal of what appears to be a downward trend regionally if only the longer records are used as a basis for evaluation. Despite significant interannual variability the date when snow cover disappears over the region appears to be reasonably well correlated spatially and temporally. The analysis also indicates that the spring melt over the North Slope of Alaska progresses from the more southerly locations of the Kuparuk River Watershed northward toward the coast (e.g., Barter Island), and melting occurs last in the vicinity of Cooper Island and BRW. This pattern of melting is very consistent with that shown by Zhang *et al.* [2000], who used AVHRR-derived albedos to show the spatial and temporal distribution of springtime snow cover north of the Brooks Range. Finally, BRW appears to be a very representative location to assess variations in the annual snow cycle associated with climate change of northern Alaska.

4. Factors That Influence the Date When the Snow Cover Disappears in Spring in Northern Alaska

[14] Two previous investigations provide clues as to why snow cover is disappearing earlier in spring over northern Alaska. Stone [1997] documented a warming trend there, most pronounced in late winter and spring. He found that at Barrow, February–May surface temperatures had increased $\sim 3^\circ\text{C}$ since 1965. Curtis *et al.* [1998], using end of season snow depth measurements, showed that snowfall over a region extending across northern Alaska into northwestern Canada had decreased. The disappearance of snow cover in spring should occur early if snow accumulation is below average and/or temperatures, particularly during spring, are above average. We hypothesize that such conditions have become more common in recent decades, which explains the observed trend in the date when the tundra becomes snow-free across northern Alaska. Figure 4 presents a comparative analysis in support of this hypothesis. Interpretation of Figure 4 requires an understanding of the annual snow cycle in this region and of the processes that influence the accumulation and ablation of snow.

4.1. Annual Accumulation and Ablation of Snow in the Vicinity of Barrow

[15] In the vicinity of Barrow most of the annual snowfall accumulates by the end of February, March tends to be dry and mostly sunny, and by mid-April the snowpack begins a fairly rapid decline [e.g., Zhang *et al.*, 1996a]. Aizen *et al.* [2000] describe the annual ablation of the snowpack at high latitudes in terms of energy exchanges. Their observations indicate that sublimation begins long before any actual melting takes place. The process is

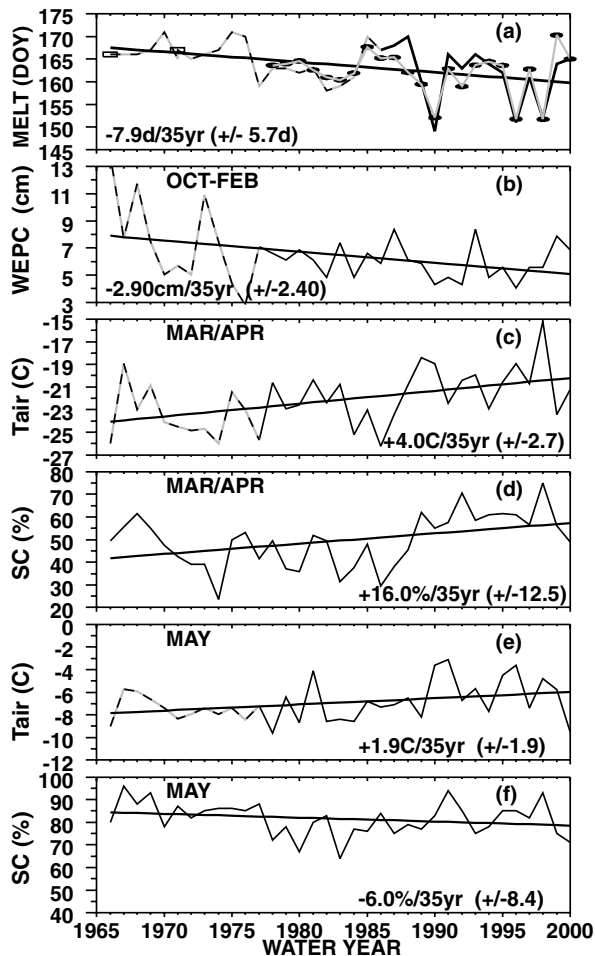


Figure 4. The 1966–2000 time series of (a) observed (from Figure 2) and modeled (ellipses) melt dates at NOAA/CMDL-BRW, (b) October–February water-equivalent precipitation, adjusted prior to 1977 (dashed curve) to account for “wind-induced undercatch,” (c) average March/April 2-m temperature (solid curve) and adjusted NWS air temperature (dashed curve), (d) average March/April total sky cover, (e) average May CMDL-BRW air temperature (solid curve) and adjusted NWS-Barrow air temperature (dashed curve), and (f) May total sky cover. Legends give results of linear fits of the respective time series with uncertainties (given in parentheses) at the 95% confidence level.

enhanced by increasing solar insolation as the season progresses and is augmented by warm-air advection from regions where snow has already melted. Aizen *et al.* [2000] found that depending on location, over 20% and as much as 60% of the snow-water equivalent of the snowpack is removed prior to the final melt period that lasts only ~ 10 days. Thus sublimation is a critical process that must be considered when assessing the annual snow cycle. Other studies have quantified sublimation rates for polar regions using various models and/or observations [e.g., Pomeroy *et al.*, 1997; Liston and Sturm, 1998; King *et al.*, 2001], reporting amounts ranging from 10 to 50% of winter snowfall totals. Pomeroy *et al.* [1997] estimate losses of 20–47% for the western Canadian Arctic. A recent estimate for the Alaskan Arctic has been made by G. E. Liston and M. Sturm (Winter precipitation patterns in Arctic Alaska determined from a blowing-snow model and snow-depth observations, submitted to *Journal of Hydrometeorology*, 2001). They estimate that along the windy coastal plain of northern

Alaska, 33% of the winter precipitation is sublimated. Sublimation varies depending on complicated interactions involving wind, relative humidity, temperature, and solar insolation. It can occur when winds are calm if relative humidity is low, but it increases nonlinearly with wind speed. Snow particles can become airborne when surface winds exceed 5 m s^{-1} . Exposing more surface area to the air enhances evaporation rates [e.g., Liston and Sturm, 1998].

[16] At BRW we find that during March and April, hourly mean wind speeds (at 10 m height) exceed 5 m s^{-1} 53% of the time; 18% of these winds exceed 10 m s^{-1} , and the average speed of winds $>5 \text{ m s}^{-1}$ is 7.9 m s^{-1} . While surface wind speeds are generally lower, it is clear that much of the time, speeds exceed the threshold associated with blowing-snow sublimation. March/April, after January/February, is also the driest period of the year at BRW, which favors higher sublimation rates. Mean daily relative humidities (with respect to water) at BRW during March and April range from ~ 78 –84% [Stone *et al.*, 1996]. Therefore, March/April sublimation rates are probably quite significant despite persistent cold temperatures that range from about -30°C to -8°C [Stone *et al.*, 1996].

[17] It is clear from the analysis of Zhang *et al.* [1996a, Figure 11] that the evolution of the snowpack at Barrow is influenced by sublimation because snow depth remains stable during March and typically begins a fairly rapid and monotonic decline during the second week in April, while snow continues to fall. On the basis of a 51-year (1950–2000) Barrow climatology (NOAA National Climate Data Center (NCDC), 2001, available at <http://www.wrcc.dri.edu/cgi-bin/cliMAIN.pl?akbarr>) the combined snowfall for March and April accounts for $\sim 20\%$ of the October through April total and yet snow depth decreases to $\sim 72\%$ of its maximum depth by the end of April, according to Zhang *et al.*'s analysis [1996a]. Compaction must account for some of the reduction in snow thickness, but sublimation probably contributes significantly. If only half the decrease in snow thickness is due to sublimation, i.e., 14%, then an approximate snow loss during March and April is $\sim 34\%$, the additional 20% being the average amount of snow that falls during these months without accumulating. It appears that the March/April period plays an important role in establishing not only the depth of the snowpack but also its snow-water equivalent prior to the final disappearance of the snow cover in spring.

[18] In the following analysis we consider separately three phases of the annual snow cycle at BRW: (1) the primary period of snow accumulation (October through February), (2) ambient conditions represented by air temperature and cloudiness during March/April that affect sublimation rates, and (3) temperature and cloudiness during May that affects the actual rate of snowmelt in its final stages. We evaluate the correlation of the BRW melt date time series (Figure 4a) with each variable during each phase to determine their relative influence on the date of snow cover disappearance.

4.2. Winter Snowfall Variations

[19] To evaluate variations in snowfall amount, we constructed a time series of the measured water equivalent precipitation (WEPC) integrated for October through February (Figure 4b). WEPC is measured using gauges of various types. Making accurate measurements of snowfall during winter in the windy environment of coastal Alaska is problematic [e.g., Black, 1954; Benson, 1982; Clagett, 1988]. The perfect gauge has yet to be constructed, but it is now widely accepted that the most reliable estimates of snowfall in windy environments are obtained from gauge systems that account for the “undercatch” of windblown snow. At BRW, wind-shielded gauges have been in use since the late 1970s as part of the U.S. Department of Agriculture’s Natural Resources Conservation Service (NRCS) network of stations [Natural Resources Conservation Service, 1994]. In our opinion, the NRCS precipitation data are currently the most reliable in the vicinity of Barrow for analyzing long-term trends. Data prior to 1977 were obtained from the NWS, where a standard 8-inch gauge has been in continuous use. Yang *et al.* [1998] recommend adjustments be made to standard gauge data

on a daily basis to account for biases due to wind-induced undercatch, wetting losses, and trace amounts of precipitation. We adopt a simpler approach. For the period 1966–1976 that precedes the availability of shielded gauge data, we apply monthly correction factors (CFs) to scale the NWS data to adjust for undercatch. The merging of these data with the NRCS time series permits an analysis of the longer-term record of snowfall amounts in the vicinity of Barrow.

[20] We first constructed separate monthly climatologies of measured precipitation using NCRS shielded gauge data from BRW (1977–1996) and of standard gauge data from NWS (1949–1996). From these we calculated the ratios of NRCS to NWS mean precipitation amounts to determine monthly CFs. For the months from October through February these are 1.70, 2.07, 3.07, 2.22, and 2.52, respectively, averaging 2.32. This is in fair agreement with a value of 2.6 given as an annual snowfall adjustment factor by Zhang *et al.* [1996a].

[21] Next, we determined a set of monthly CFs from the analyses of Yang *et al.* [1998], presented in the form of graphical comparisons of standard gauge results and values of precipitation adjusted for wind-induced undercatch and other errors. Results are given for 1982 and 1983, years at Barrow that were relatively wet and dry, respectively. Monthly adjustment factors did not vary greatly from one year to the other. We averaged the values for the two years to estimate the following October through February ratios: 1.68, 2.52, 2.14, 1.98, and 1.98, respectively, averaging 2.05. Various other adjustment factors have been reported in the literature but in general, these indicate that shielded gauges located in Arctic environments catch at least twice the amount of snow collected by the standard NWS 8-inch gauges. There is no correct or true value when correcting standard gauge data retrospectively. For the purpose of this study the average of our climatologically determined CFs and the mean 1982/1983 values derived graphically from Yang *et al.*'s [1998] analysis are used to scale the 1966–1976 NWS data. Adjustments are applied on a monthly basis before the seasonal integrations shown in Figure 4b are computed. Although individual monthly data are subject to error due to variations in wind speed, no significant bias should result using our approach. We are confident that this merged time series captures the long-term trend in snowfall that we wish to evaluate. Moreover, the detailed analyses of variations in snowfall (measured as water equivalent precipitation) that follow focus on recent years for which shielded gauge data are available.

[22] A 36% decrease in October–February snowfall over the 35-year period is indicated by the linear regression shown in Figure 4b. This is in general agreement with the results of Curtis *et al.* [1998] who document declining snow depths in the region since the mid-1950s. In a recent summary of Arctic snow cover variations, Serreze *et al.* [2000] update earlier satellite records that began in 1972 and show that NH snow cover has decreased by $\sim 10\%$, largely due to spring/summer deficits since the mid-1980s. Canadian station records dating from the 1940s also show decreased snow depths during spring, and other records show diminished depths during winter over European Russia since the turn of the century [Serreze *et al.*, 2000]. In some regions of Russia, however, snow depths have increased [Ye *et al.*, 1998]. Still, Serreze *et al.* [2000, Figure 10] conclude that the “common thread” between the various studies of the seasonality of NH snow cover is an indication of “an overall reduction in spring snow cover.” Over northern Alaska and northwestern Canada, this appears to be due to diminished snowfall in recent decades [Curtis *et al.*, 1998]. Diminished snowfall at high northern latitudes is inconsistent with climate simulations that show increased precipitation in response to enhanced greenhouse warming, expected in the Arctic if global warming occurs [Houghton *et al.*, 1996]. This apparent paradox needs to be further investigated.

4.3. Spring Temperature and Sky Cover Variations

[23] Figures 4c and 4d are time series of average March/April temperatures (T) and total sky cover (SC), analyzed to evaluate variations in ambient conditions prior to the final period of snowmelt that begins in May. As emphasized in section 4.1, sublimation can be very significant during this period. Although we cannot quantify the variations in sublimation amounts at BRW year-to-year, we can evaluate variability in temperature and cloudiness that influence sublimation rates. The influence of clouds on sublimation has not been evaluated to our knowledge but is potentially important because clouds enhance atmospheric emissions of thermal radiation quite dramatically. During March/April the downward flux of longwave (LW) radiation can increase by as much as 100 W m^{-2} during transitions from clear to overcast conditions [Stone *et al.*, 1996; Stone, 1997]. Because the surface absorbs $\sim 98\%$ of this energy, snow (skin) temperatures warm by as much as 8° – 12°C when clouds form or advect over the surface. Although upward LW fluxes increase in response to the warmer snow temperatures, the net LW irradiance increases by 30 – 50 W m^{-2} under such conditions. These LW perturbations are independent of solar geometry, so their effect persists day and night as long as the clouds are present. This represents a large positive radiative forcing that may accelerate sublimation. Even when daily average solar fluxes reach 250 W m^{-2} at the end of April, the amount of solar energy absorbed by snow is $< 50 \text{ W m}^{-2}$ because the surface albedo is high, ≈ 83 – 85% . Because thermal forcing by clouds exceeds their negative albedo effects, even in late May, clouds probably modulate seasonal ablation rates significantly. There is theoretical evidence of this as well. Zhang *et al.* [1996b], on the basis of radiative transfer calculations, show that the onset of the spring melt can begin as much as a month earlier under conditions of low stratus cloud cover versus when skies are clear. We speculate that clouds affect snow morphology as well because thermal-induced microphysical changes at the surface may alter snow crystal habit. These changes in the microphysical properties of the snowpack in winter and early spring may affect the rate of melt later on. In the future, investigations of Arctic ablation rates should include careful assessments of these LW (thermal) effects of clouds because these are potentially more important than solar insolation in controlling ablation rates, especially during winter and early spring.

[24] In the present study we restrict our analysis to air temperature and total sky cover. The temperature data (Figure 4c) are from CMDL-BRW with the exception of the period 1966–1977 which is from the NWS. Following a similar approach to the one used to scale precipitation data (see section 4.2), we adjusted for small biases found between the data sets. We determined the average differences between the NWS and BRW March and April temperatures on the basis of a 20-year overlap period (1977–1996) and added these differences to the 1966–1977 NWS monthly temperatures to produce a consistent time series for analysis. On average, NWS March and April monthly mean temperatures were found to be 0.49° and 0.35°C warmer, respectively, than at BRW. All SC observations for March and April (Figure 4d) were made by trained NWS observers and were obtained from the NCDC in Asheville, North Carolina. Similar analyses of May temperatures and sky cover are presented in Figures 4e and 4f. May temperatures from the NWS (1966–1977) showed only a 0.22°C warm bias that was accounted for when merging the time series shown in Figure 4e.

5. Trend and Correlation Analyses of Factors Affecting Snowmelt at Barrow

[25] The record of BRW melt date (Figure 4a) was cross-correlated with each variable shown in Figures 4b–4f, and the respective time series were fitted linearly to assess long-term trends. Regression results are given in Figure 4 legends on the

Table 1. Listing of Correlation Coefficients That Relate Paired Time Series That Cross-Reference With Figure 4a

Correlation (r) Variable Pair ^a	Figure 4 Reference	1966–2000 (r_{35} years)	1978–2000 (r_{23} years)
Melt: WEPC	4a: 4b	+0.22	+0.51
Melt: $T_{\text{Mar/Apr}}$	4a: 4c	–0.51	–0.59
Melt: $SC_{\text{Mar/Apr}}$	4a: 4d	–0.30	–0.36
$T_{\text{Mar/Apr}}$: $SC_{\text{Mar/Apr}}$	4c: 4d	+0.69	+0.70
Melt: T_{May}	4a: 4e	–0.35	–0.30
Melt: SC_{May}	4a: 4f	–0.29	–0.28
T_{May} : SC_{May}	4e: 4f	+0.47	+0.67
Equation (1): melt	4a ^b : 4a	–	+0.85 (3.2) ^c
Equation (2): melt	equation (2) not shown	–	+0.88 (3.3) ^c

^a WEPC, water equivalent precipitation; T , temperature; SC, total sky cover.

^b Equation (1) results shown as solid ellipses in Figure 4a.

^c Standard deviation of multiple regression (in days).

basis of the 95% confidence level. Table 1 lists correlation coefficients (r) for relevant pairs of variables. Correlations were computed for the 35-year record and also the recent 23 years (1978–2000), the period for which we have the most reliable gauge measurements of snowfall (WEPC) and temperature. Cross-referencing Table 1 and Figure 4, note that melt dates are positively correlated with integrated October–February WEPC that has decreased and are anticorrelated with March/April and May temperatures and sky cover that show increases, with the exception of May SC that shows a slight but statistically insignificant decrease. Also, note that air temperatures are positively correlated with sky cover because clouds enhance thermal radiation throughout the winter and spring, as discussed in section 4.3. Finally, note that the correlation between melt date and WEPC is much higher for the period 1978–2000 than for 1966–2000. The 1978–2000 correlation is probably the more valid analysis because we have greater confidence in the shielded gauge data used in the calculation.

[26] To further assess the relationship between the factors that influence the eventual snowmelt, we developed a multiple regression model that can be used to predict the date when the snow disappears at BRW (equation (1)). The melt date DOY, D , can be estimated by combining terms of October–February snowfall (WEPC, W), March/April temperatures (T) and March/April total SC, S , as follows:

$$D \approx 14.0W - 0.95W^2 - 7.6T - 0.13T^2 + 0.23S. \quad (1)$$

The regression was evaluated only for the period 1978–2000 to assure that the most reliable input data were used. Figure 4a shows that predicted melt dates (ellipses) are well correlated with the observations: $r = 0.85$. This simple empirical relationship explains 72% of the variance in snowmelt date. Although (1) is applicable only for BRW, it seems plausible that similar expressions with different sets of coefficients could be developed for other tundra sites if long-term values of the input variables and concurrent observations of the date of snow disappearance are available. This empirical approach may have practical hydrological and biogeochemical applications because a melt date prediction can be made several weeks in advance (as of 1 May each year). In this case the standard deviation of prediction is 3.2 days.

[27] Because ambient conditions immediately preceding and concurrent with the final stages of snowmelt in spring can accelerate or delay the melt, we developed a similar regression model that includes terms for May temperatures (Figure 4e) and sky cover (Figure 4f). The result is

$$D \approx 12.1W - 0.77W^2 - 6.9T - 0.12T^2 + 0.12S - 2.3T_{\text{May}} - 0.16T_{\text{May}}^2 + 0.20S_{\text{May}}, \quad (2)$$

where the last three terms represent the May input variables. Including these terms, as expected, increases the correlation between observed and predicted melt dates: $r = 0.88$; thus 77% of the variance is now explained. However, the standard deviation of prediction is slightly greater, 3.3 days. Of course, by including May inputs, any lead time in forecasting the melt date is reduced by at least 1 month, and sometimes snowmelt is complete before the end of May (see Figure 4a). We believe that more accurate forecasts of melt dates are possible by modifying (1) to include an index of March/April sublimation rates and also of the March/April snowfall amounts to account for anomalously high or low snowfall during these months. On the basis of the 1978–2000 NRCS record of BRW snowfall, the average March/April WEPC is ~ 2 cm, or $\sim 20\%$ of the October–April total. This is in agreement with the 30-year NWS climatology mentioned in section 4.1. The standard deviation of March/April WEPC is ~ 0.8 cm with a range between ~ 0.04 and ~ 3.7 cm. Thus, in 95% of the years considered, the relative uncertainty in using only October–February versus October–April WEPC is $< 20\%$ assuming that an average October–February amount (~ 7 cm; see Figure 4b) is used as a reference. Such variations should not influence the prediction of melt date significantly. If however, snowfall during October–February is anomalously low and the March/April snowfall is anomalously high, then (1) would fail to give a good estimate of the melt date. Similarly, if the weather during May is abnormally cold or warm, overcast or clear, wet or dry, then using (1) to forecast the melt date is subject to large uncertainties. Despite these obvious limitations, Table 1 together with (1) serve to demonstrate that in most years the amount of October–February snowfall and ambient conditions during March/April combined influence the date of snow disappearance at BRW more than do May weather conditions alone.

6. Influence of Circulation on the Date of Snow Disappearance in Northern Alaska

[28] Stone [1997] documented how shifts in circulation patterns influence the temperature regime of northern Alaska. He showed that variations in atmospheric temperatures and clouds at Barrow were correlated with the frequency and intensity of southwesterly winds aloft. Airflow to BRW was found to vary with the relative position and intensity of two pressure systems, the Aleutian Low (AL) and what we refer to as the Beaufort Sea Anticyclone (BSA). Here we extend that analysis to evaluate how snowfall is affected by changes in synoptic patterns that are dominated by these two pressure centers.

[29] Our approach is similar to that of Harris and Kahl [1994] whereby the frequency and transit times of back trajectories passing through defined source regions to BRW are quantified. To evaluate flow associated with the BSA and AL, we define Arctic and North Pacific source regions, respectively, that approximately encompass the centers of these pressure systems. These regions are lightly

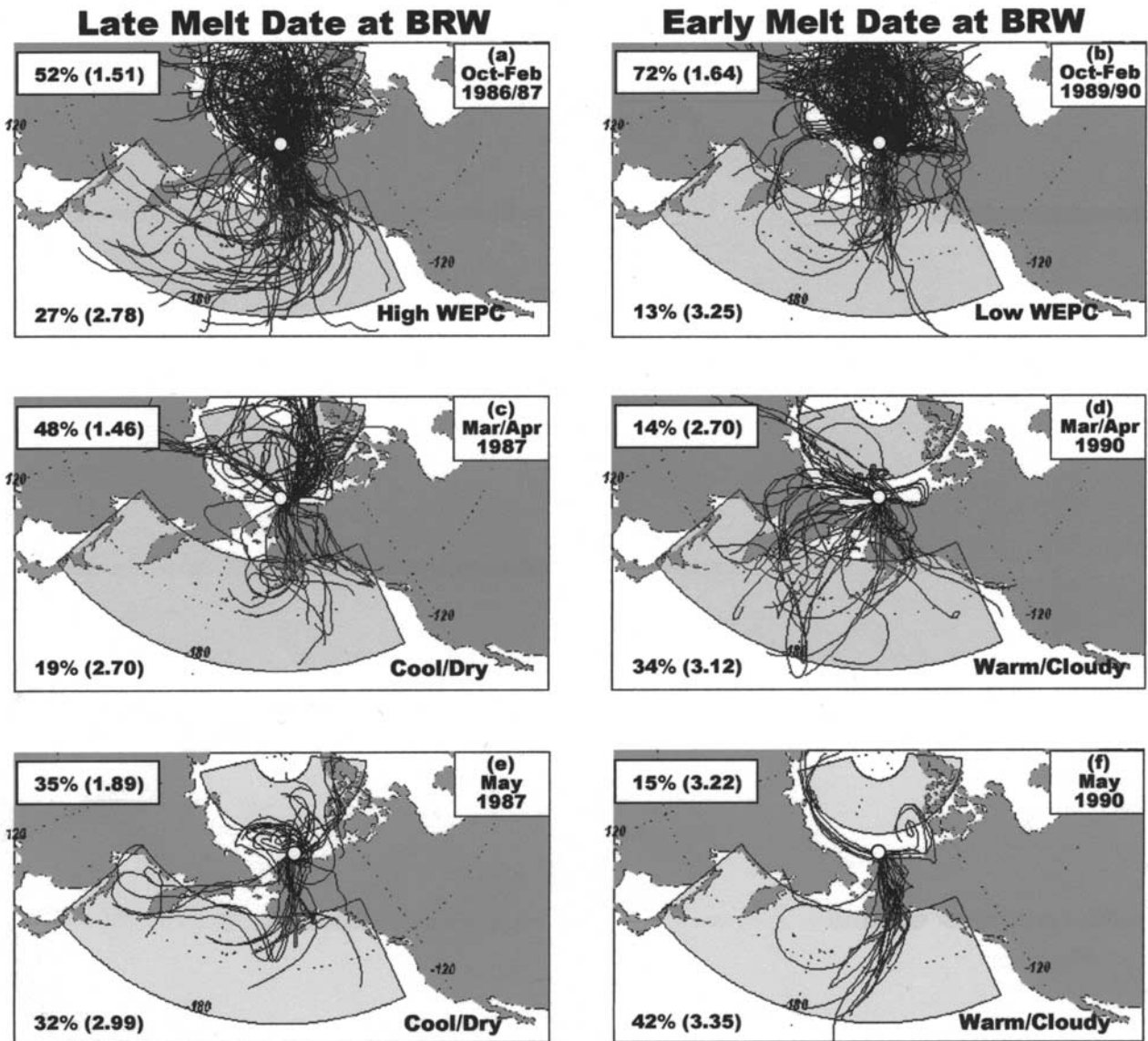


Figure 5. Trajectory analyses relative to NOAA-CMDL-BRW, showing all individual 1500-m back trajectories emerging from defined source regions (light shading) in the North Pacific and Arctic Ocean. BRW is indicated by the circle where all trajectories meet. Analyses are for (a) October–February 1986/1987, (b) October–February 1989/1990, (c) March/April, 1987, (d) March/April 1990, (e) May 1987, and (f) May 1990. The percent frequency of transport and average transit time from each source region (in days) are indicated in the legends: The upper left legend relates to northerly flow from the Arctic, and the lower left legend relates to southerly flow from the North Pacific region. As indicated, the melt date at BRW was late in 1987 relative to 1990 due to higher October–February snowfall (measured as water equivalent precipitation (WEPC)), followed by cool/dry weather conditions during March/April and May of that year. These contrasts in weather are evident in the time series presented in Figure 4.

shaded in Figure 5, which shows examples of the trajectory analyses that were conducted for the years 1986–2000. In the following discussion, “years” refer to “water years” that span from the autumn of one year through the spring of the following year, October to May for purposes of this analysis. The NOAA/CMDL isentropic transport model was used to calculate twice daily (0000 and 1200 UT), 5-day back trajectories using gridded upper air data supplied by the European Centre for Medium Range Weather Forecasts. Although individual trajectories are subject to uncertainties arising from the interpolation of sparse meteorological data, earlier studies show that averaged results represent general flow patterns reasonably well [e.g., Harris and Kahl, 1994].

[30] We analyzed back trajectories calculated for an arrival altitude of 1500 m in conjunction with 850 hPa geopotential height fields. At BRW this level generally tops the surface inversion layer where the advection of heat and moisture plays an important role in cloud-radiative and dynamical processes [Stone, 1997]. We assume that a source region influences BRW if a back trajectory passes through some portion of that region within the 5-day period. To evaluate transport that affects winter snowfall, October–February trajectories and geopotential fields were analyzed. A similar analysis was made to assess how synoptic patterns influence March/April and May temperatures and snow cover. Evaluations are based on the percent frequency of flow from a particular region by season or

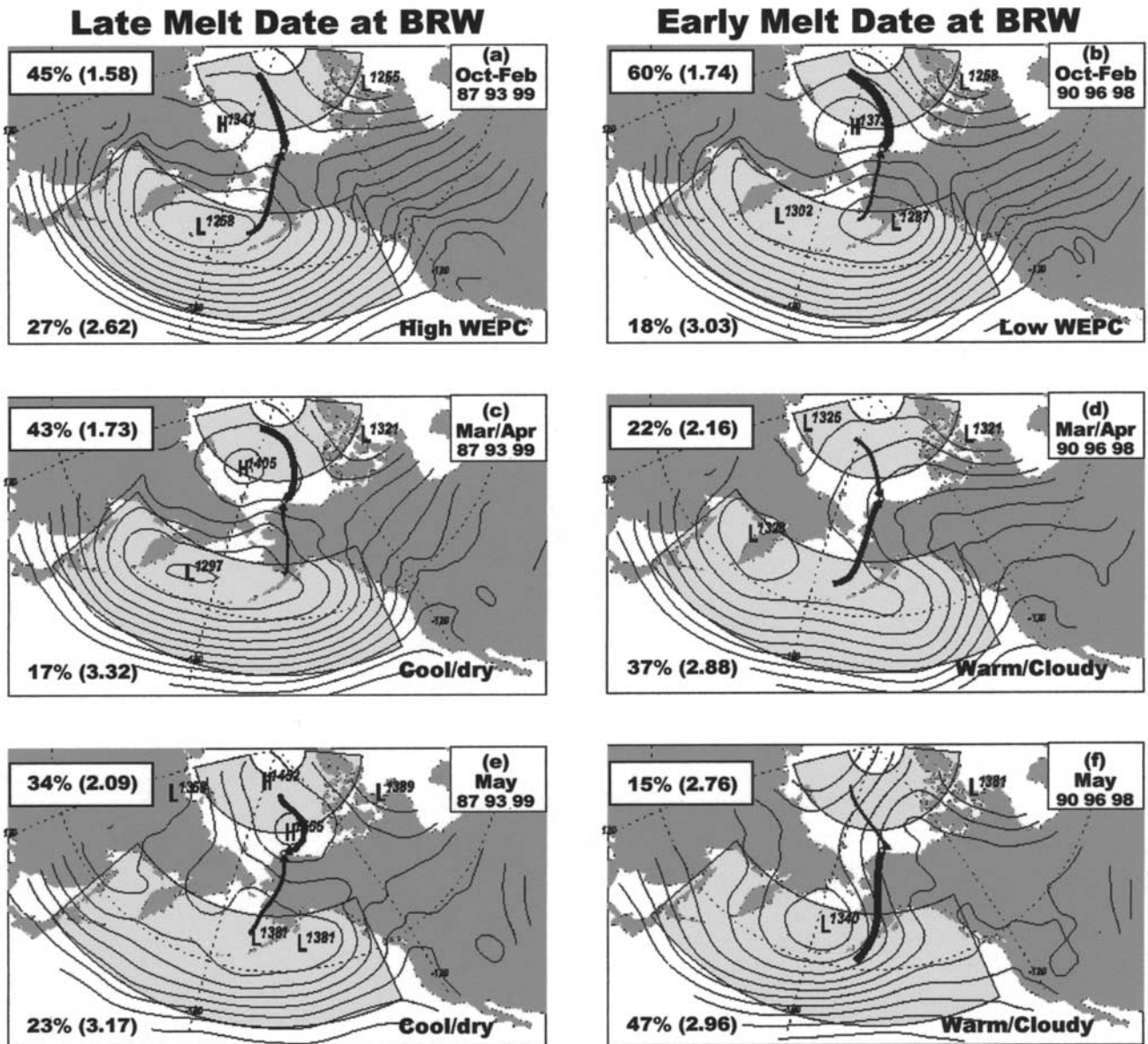


Figure 6. Averaged, 1500-m back trajectories relative to the NOAA-BRW and corresponding 850-hPa geopotential height fields for (a) October–February 1987, 1993, and 1999, (b) October–February 1990, 1996, and 1998, (c) March/April 1987, 1993, and 1999, (d) March/April 1990, 1996, and 1998, (e) May 1987, 1993, and 1999, and (f) May 1990, 1996, and 1998, showing the seasonal average, 5-day airflow from source regions indicated as lightly shaded areas. The percent frequency of transport and average transit time from each source region (in days) are indicated in the legends: The upper left legend relates to northerly flow from the Arctic source region, and the lower left legend relates to southerly flow from the North Pacific source region. The thickness of trajectories is proportional to their frequency, and their lengths are inversely proportional to average speed along track. These average trajectories represent the mean flow of all individual trajectories from the respective regions over each period indicated in the upper right hand legend. Results are derived from multiple-year analyses such as those shown in Figure 5. As indicated, the melt date at BRW was late in 1987, 1993, and 1999 relative to 1990, 1996, and 1998 due to higher October–February snowfall (measured as WEPC), followed by cool/dry spring weather conditions. These conditions are contrasted in the time series shown in Figure 4.

month and on the average transit time (in days) that it takes an air parcel to reach BRW once it emerges from a particular region.

[31] Figures 5a, 5c, and 5e characterize flow patterns for a year when the snowmelt at BRW was late (1987), and Figures 5b, 5d, and 5f show patterns for a year when the snowmelt occurred early (1990). Each panel shows all individual back trajectories emerging from the defined regions during periods that correspond with those evaluated in Figure 4. These are labeled Oct–Feb, Mar/Apr, and

May in the upper right-hand legends. The upper and lower left-hand legends give percentages and average transit times associated with flow from the northern and southern source regions, respectively. Referring again to Figure 4, note that October–February 1986/1987 was a relatively snowy season with WEPC of ~9 cm, whereas October–February 1989/1990 was a year of low WEPC (~4 cm). Note also that March/April and May 1987 were relatively cool and cloudy and March/April and May 1990 were quite warm with

moderately high SC. As discussed above, the combination of these factors very likely contributed to a late melt date in 1987 and an early one in 1990. A close inspection of Figures 5a and 5b reveals a flow pattern that favors high (low) snowfall during October–February. Similarly, Figures 5c and 5d and Figures 5e and 5f show patterns that favor cool/clear (warm/cloudy) conditions at BRW during March/April and May, respectively. The frequency distribution and transit times associated with the trajectory groupings indicate that high snowfall (Figure 5a) occurs when a significant percentage (27%) of the flow is from the North Pacific and transit times are relatively fast (2.78 days). Southerly flow during October–February transports heat and moisture to northern Alaska that enhances snowfall there.

[32] Low snowfall (Figure 5b) occurs when a lower percentage (13%) of the trajectories from the south reach BRW and the flow is weak (transit time of 3.25 days). Instead, a high percentage (72%) of trajectories came from the Beaufort Sea region. This northerly flow of cold, dry air tends to block the advection of moist air from the Aleutian source region, resulting in diminished snowfall north of the Brooks Range.

[33] Similarly, during March/April and May, conditions tend to be cooler and drier if the dominant flow is from the north (Figures 5c and 5e), but warm and cloudy if southerly flow prevails (Figures 5d and 5f).

6.1. Composite Multiyear Flow Patterns

[34] We take this analysis one step further in Figure 6 by averaging multiple years to contrast flow patterns that affect the timing of snowmelt at BRW. Three-year composites are presented for each case. Years were selected that combine high (low) snowfall in October–February with cold/clear (warm/cloudy) March/April seasons that led to late (early) disappearance of snow at BRW. The May analyses are also included to assess whether or not the March/April patterns persist during the final stage of snowmelt. We superimpose the mean flow, represented by averaged back trajectories, onto the mean 850-hPa geopotential height fields that are roughly concurrent with trajectory altitude (1500 m). This shows the relationship of transport pathways and synoptic patterns, particularly the position and intensities of the AL and BSA pressure centers.

[35] Figure 6 contrasts composite analyses for 3 years of early snowmelt, 1990, 1996, and 1998 (Figures 6b, 6d, and 6f), with 3 years when the melt occurred much later, 1987, 1993, and 1999 (Figures 6a, 6c, and 6e). As was indicated in Figure 4, these early (late) melt seasons were associated with below (above) average October–February snowfall and above (below) average March/April and May temperatures. Figure 6b shows that during October–February of 1990, 1996, and 1998, 60% of all trajectories reaching BRW emerged from the northern region and only 18% emerged from the south. This pattern inhibits snowfall because northerly winds are very cold and dry during winter when extensive sea ice cover limits the supply of moisture. High pressure north of Barrow blocks the advection of warm, moist air from the south. Figure 6d shows that by March/April of these years the pattern had essentially reversed. More vigorous flow from the Bering Sea is dominant, a pattern favoring the advection of heat and moisture to northern Alaska that we know enhances cloudiness and results in warmer conditions there. Figure 6f shows that on average, patterns established during March/April persisted through May of these years with an even greater contrast between the southerly and northerly flow frequencies. Again, warm-air advection reaches BRW from the Aleutian region. By this time of year much of Alaska is snow-free, so air transported northward may be further warmed due to positive radiative feedbacks from the warm underlying surface. In addition, adiabatic warming of the air when descending from the Brooks Range may promote warmer, drier conditions along the northern coast. Average temperatures for May 1990, 1996, and 1998 were 2.3°C warmer than during May 1987, 1993, and 1999 (−3.9° versus −6.2°C) attributed to these differing synoptic patterns. In 1990, 1996, and 1998, anomalously warm

May temperatures most certainly contributed to an earlier snowmelt at BRW.

[36] Generally, the seasonal patterns for 1987, 1993, and 1999 (Figures 6a, 6c, and 6e) are opposite of those noted for 1990, 1996, and 1998. Greater October–February snowfall was associated with more rapid and frequent flow from a deeper AL centered over the Bering Sea. Cooler March/April conditions were attributed to a two-fold increase in northerly flow associated with an intense BSA centered northwest of BRW, effectively blocking the flow of warmer air from the south. Also, to some extent, these March/April patterns persisted into May. The high-pressure system that shifted into a position north of Barrow continued to inhibit the flow of air from the south. The pattern contrasts with the composite for May 1990, 1996, and 1998 that shows a complete absence of high pressure north of Alaska, a continuation of the March/April pattern of those years.

[37] In summary, years with below (above) average snowfall at BRW are influenced predominantly by flow from the Arctic (Aleutian) source region, while warm (cool) spring conditions occur if flow from the Aleutian (Arctic) region is favored. The juxtaposition and relative intensities of the AL and BSA determine advective patterns that influence the North Slope weather seasonally and in turn, influence the timing of spring snowmelt.

[38] While the above analysis focused on only 6 years that were selected to contrast extremes of snowfall and temperatures, the manner in which we quantify the frequency of flow and transit times from defined source regions lends itself to performing a time series analysis of these transport characteristics. We investigated the trend in the frequency of flow from the Aleutian source region for the October–February period, 1986–2000, and correlated the measured snowfall for the same months to further assess whether changes in circulation can explain the decrease in winter snowfall at BRW. The frequency of southerly flow showed only a slight downward trend that is not statistically significant. However, the correlation (r) between snowfall amount and the frequency of trajectories reaching BRW from the North Pacific region was +0.66, indicating that the interannual variability in winter snowfall amount is partly explained by variations in the AL. We also found that the transit time from the North Pacific source region has increased and is significantly anticorrelated with flow frequency ($r = -0.88$). That is, flow from the North Pacific appears to have weakened and become less frequent during October–February over the last 15 years. As a consequence, winter snowfall has decreased north of the Brooks Range. There is evidence of this in Figures 5b and 6b compared with Figures 5a and 6a that show diminished flow from the North Pacific region during years of low snowfall there.

6.2. Influence of Planetary Modes of Circulation on Factors Affecting the Annual Snow Cycle in Northern Alaska

[39] The weakening of the Aleutian Low during October–February discussed in section 6.1 may be related to a rise in the Arctic Oscillation (AO) index [Thompson and Wallace, 1998]. The AO is thought to be the leading mode of Northern Hemispheric, wintertime circulation changes. High indices are associated with anomalously low pressure over the central Arctic and anomalously high pressure south of $\sim 50^\circ$ N latitude where the AL is centered (see Figure 6). To determine whether the variations of winter snowfall and spring temperatures that influence the melt date at BRW are associated with the AO, we correlated these variables with indices derived from the monthly AO index values of Thompson and Wallace [2000]. October–February WEPC and March/April and May temperatures and sky cover were separately correlated with AO indices averaged over October–February (AO_{ONDJF}) and March/April ($AO_{\text{Mar/Apr}}$) periods, respectively. We performed similar analyses using the Aleutian Low Pressure Index (ALPI) of Beamish et al. [1997]. The ALPI gives the relative intensity of the Aleutian Low for December–March, with

positive index values reflecting a more intense AL. We found no significant correlation between our variables with any of these indices. Only weak positive correlations between March/April temperatures and sky cover and AO_{NDJF} were found ($r = 0.31$ and 0.32 , respectively). This suggests that the warmth and enhanced cloudiness observed at BRW during March/April might be associated with the positive phase of the AO during winter, but only marginally. Future investigations of how northern Alaskan climate varies with the North Pacific Index [e.g., *Trenberth and Hurrell*, 1994] and the Pacific Decadal Oscillation [*Bond and Harrison*, 2000] should be made because these indices also relate to variations in the Aleutian Low that are known to have a significant affect on the variability of climate in the North Pacific [*Overland et al.*, 1998].

7. Response of the Surface Radiation Budget and Temperature to Variations in Melt Date

[40] We can estimate the perturbation in the net surface radiation budget (NSRB) caused by an early melt from continuous radiation measurements made at NOAA/CMDL-BRW. Table 2 quantifies the average June and seasonal (May–August) total radiative energy received at the surface for 3 years of early snowmelt compared with 3 years when the melt occurred ~ 2 weeks later. On a seasonal basis the NSRB increases by an average of 8 MJ m^{-2} ($\sim 1\%$) for each day the melt advances. Thus, for an 8-day advance (Figure 3a), $\sim 64 \text{ MJ m}^{-2}$ of additional radiative energy is absorbed by the surface, most of this during early June when the albedo decreases so rapidly (Figure 1a). We agree with *Maykut and Church* [1973, p. 626]: “the most significant factor influencing the magnitude of the yearly net radiation total is the date when snowmelt is completed.” As the surface absorbs this additional energy it may be redistributed in complicated ways that involve ground storage, sensible and latent heat exchanges between the surface and atmosphere, and advective processes that can distribute the radiation gain to other regions. Although we are unable to quantify these processes, some degree of atmospheric warming ultimately results from enhanced solar absorption at the surface. *Groisman et al.* [1994] suggest that radiative forcing due to a decrease in surface albedo has contributed to the recent warming over NH land areas. Also, *Aizen et al.* [1997] suggest that a feedback involving a long-term decrease in snowfall over the Tien Shan of Russia has contributed to rising June–August temperatures in that region. Our own analysis (Table 2) suggests that June temperatures at BRW rise by $\sim 1^\circ\text{C}$, on average, in response to a 2-week advance in the melt date there, and slightly warmer temperatures may persist through July/August. Our limited samples show large variations, however, prohibiting an accurate assessment of this temperature-albedo feedback, and we do not take into account other factors such as cloud variations, turbulence, or large-scale advection. We can only conclude that

the radiative perturbation caused by an early melt is very significant in the vicinity of Barrow. Compared with an annual NSRB at BRW of $\sim 470 \text{ MJ m}^{-2}$ [*Stone et al.*, 1996], an 8-day advance in melt results in a 12–14% increase, or $\sim 2 \text{ W m}^{-2}$ of thermal forcing on an annual basis. Hemispheric scale estimates of the radiative effect of diminished snow cover have also been made. Over northern extratropical land (NEL) areas, *Groisman et al.* [1994] report an increase in net radiation of 0.9 W m^{-2} (in spring, 2.6 W m^{-2}) from 1979 to 1990 due to a retreat of snow in spring. They found a corresponding increase in the annual mean air temperature of $\sim 1.0^\circ\text{C}$ over the NEL that they attribute in large part to a temperature-albedo feedback. *Kuang and Yung* [2000] used monthly reflectivity data from Nimbus 7 (Total Ozone Mapping Spectrometer) to assess albedo decreases associated with reduced snow cover over the Northern Hemisphere. Their estimate of the increase in shortwave heating during spring due to diminished snow cover was $\sim 2 \text{ W m}^{-2}$ ($\sim 2.6 \text{ W m}^{-2}$ during April and May) from 1979 to 1991. While these sound like small perturbations, it must be noted that only a 1.0 W m^{-2} increase in net surface radiation can increase air temperature by $\sim 0.6^\circ\text{C}$ [e.g., *Ramanathan et al.*, 1989].

8. Conclusions and Final Remarks

[41] Variations in the annual distribution of snow cover over the northern high latitudes have a significant impact on the surface radiation budget (SRB) due to changes in albedo. In particular, the timing of snow disappearance in spring accounts for much of the interannual variability in the SRB that in turn, influences mean annual temperatures. Concerns about a positive temperature-albedo feedback causing an acceleration of Arctic warming as global temperatures increase have prompted many investigations of how snow cover variations impact the climate of the northern high latitudes. We have assimilated a 35-year data set of variables that influence the annual accumulation and ablation of snow in northern Alaska and have performed a number of empirical analyses that reveal some interesting features of the annual snow cycle and how and why it varies. The date of snow disappearance in spring that we refer to as melt date is a good indicator of climate change. Melt date influences the regional radiation balance and temperature regime and consequently influences biogeochemical cycles that are sensitive to the presence or absence of snow, solar insolation, variations in soil moisture, etc. The timing of snowmelt in spring in the Arctic is the most significant event of the year in terms of radiative forcing, hydrological impacts, and biological processes, all of which respond to the dramatic decrease in albedo when snow melts (Figure 1). It is imperative to understand what physical mechanisms determine the spatial and temporal distributions of snow cover. Furthermore, we need to be able to distinguish internal from external, i.e., natural from anthropogenic, causes of any future changes in snow cover.

[42] Using an assimilation of radiation and ancillary data, primarily from the NOAA/CMDL Barrow Observatory (BRW), we document changes in melt date that have occurred over the past 35 years (Figure 3), identify primary factors that influence the annual snow cycle of northern Alaska, and provide an explanation for an observed trend toward an earlier spring melt in the region. We reach the following conclusions.

[43] On average, the spring snowmelt in northern Alaska has advanced by ~ 8 days since the mid-1960s (Figure 3a). We attribute the trend to changes in synoptic patterns that have diminished winter snowfall and have favored warmer conditions in spring. Time series of these key variables are shown in Figure 4. *Brown and Braaten* [1998] also attribute decreases in snow cover (over northern Canada) to “major shifts in atmospheric circulation.” Using back trajectory analyses that were correlated with specific seasons and using years of early versus late snowmelt at BRW, we show that certain flow patterns during winter and spring can explain much of the interannual variability in melt date (Figures 5

Table 2. Comparison of Net Surface Radiation Budget and 2-m Temperatures for Early Versus Late Years of Snowmelt at NOAA/CMDL-BRW^a

Years Sampled	Late Melt Date	Early Melt Date
	1992, 1999, 2000	1990, 1996, 1998
Melt date, DOY ^b	164 (0.8)	150 (0.8)
June NSRB, ^c MJ m^{-2}	306 (2)	385 (7)
May–August NSRB, MJ m^{-2}	860 (17)	970 (43)
June $T_{2\text{m}}$, $^\circ\text{C}$	0.9 (0.59)	1.8 (0.36)
July/August $T_{2\text{m}}$, $^\circ\text{C}$	3.3 (0.62)	3.6 (0.87)

^a Standard deviations given in parentheses.

^b Day of year.

^c Net surface radiation budget.

and 6, with reference to Figure 4, and Table 1). In particular, the positions and relative intensities of the Aleutian Low (AL) and Beaufort Sea Anticyclone (BSA) appear to influence seasonal variations in snowfall amount and the springtime temperature regime of northern Alaska. While it appears plausible that variations in these pressure centers are related to the Arctic Oscillation (AO) [Thompson and Wallace, 1998], we did not find significant correlations between variables that affect the annual snow cycle and indices of either the AO or the AL. It may be that the BSA, which is in closer proximity to Alaska's North Slope than the AL, is the dominant system. The presence (absence) of the BSA appears to block (permit) intrusions of heat and moisture into the region from the North Pacific that influence North Slope snowfall and temperatures quite significantly. Further investigations of how changing modes of planetary-scale circulation affect the NH annual snow cycle are recommended.

[44] The annual net radiative forcing associated with an 8-day advance in melt date at BRW (Figure 3a) is $\sim 2 \text{ W m}^{-2}$. However, the most dramatic increase ($>150 \text{ W m}^{-2}$ on a daily basis) occurs immediately following the disappearance of snow when albedo drops from over 75% to $\sim 17\%$ in less than a week. Perturbations of this magnitude over a large region of the Arctic have most likely contributed to the recent warming over NH land areas [e.g., Kuang and Yung, 2000; Aizen et al., 1997; Groisman et al., 1994]. It also appears that an earlier snowmelt promotes an earlier onset of ice melt as evidenced by the correlation between the BRW and Isaktoak records shown in Figure 3a. The onset of ice melt is delayed to some extent until the overlying snow melts. Therefore the depth of snow on sea ice at the beginning of the ablation period may be an important factor that controls the timing of ice melt and should be considered when investigating variations in sea ice extent and concentration. It is possible that diminished regional snowfall [Curtis et al., 1998] has contributed to recent reductions in sea ice cover [e.g., Maslanik et al., 1999; Maslanik et al., 1996] directly, by allowing for an early onset of ice melt, and/or indirectly, by enhancing warm-air advection from southern land areas that became snow-free earlier in the season [e.g., Aizen et al., 2000]. Aizen et al. found that when snow cover in southern regions of Eurasia melted early in the spring, the northward advection of warm air intensified the ablation of the remaining snow. It is most likely that the ablation of snow and ice offshore is similarly enhanced when the snow cover over tundra regions disappears early.

[45] There are many other consequences of an earlier spring snowmelt over the high northern latitudes discussed in the literature. These include a lengthening of the active growing season [Myneni et al., 1997] and associated changes in the annual cycles of two important greenhouse gases, CO_2 [e.g., Keeling et al., 1996; Oechel et al., 1995] and methane [e.g., Zimov et al., 1997]. Changes in the sources and sinks of these gases have other implications in terms of feedback mechanisms that affect atmospheric warming. Permafrost is also thawing [Osterkamp and Romanovsky, 1999]. Because of these changes, plant and animal habitats, and ultimately the productivity of traditional fishing and hunting grounds, are impacted. Thus variations in the annual distribution of snow over high-latitude land areas have far-reaching implications, both in the context of global warming and in biogeochemical cycles. There is valid concern that an amplification of global warming in the Arctic will have a major effect on its ecosystems. Continued Arctic-wide monitoring of the causes and effects of variations in snow cover is essential if a better understanding of anthropogenic climate forcing is to be gained. Unfortunately, there will always be a dearth of in situ data to analyze. Therefore advances in remote sensing techniques are essential for monitoring variations in snow cover on a panarctic scale. Multispectral satellite data should be exploited for this purpose, providing that appropriate verifications of retrieval algorithms are made on the basis of surface observations [e.g.,

Zhang et al., 2000]. Similarly, further improvements in regional climate models, verified using observational data, must be made to better simulate variations in snow cover [e.g., Liston and Sturm, 1998]. The NOAA/CMDL-BRW observatory, in particular, should be a focal point for such investigations because it is a representative site for evaluating climate change in this region of the Arctic. In addition, there exists a baseline of long-term ancillary observations from NOAA/CMDL and NWS that can be used as a reference when making future assessments of climate change there.

[46] **Acknowledgments.** We received support from the International Arctic Research Center (IARC) and the Cooperative Institute for Arctic Research (CIFAR), University of Alaska, Fairbanks. NOAA/CMDL, Boulder, provided facilities and data access. We are grateful to G. Maykut for providing the historical radiometric data used in Figure 2 and to the NWS, NSIDC at CU-Boulder, G. Divoky, D. Kane, J. Foster, and C. George for providing data used in Figure 3a. R. McClure provided the BRW NCRS precipitation data. B. Halter and T. Mefford made the estimates of melt dates from temperature records. E. Rice assisted with the trajectory analysis, and D. Chao assisted with graphics. We thank D. Endres and M. Gaylord for their ongoing efforts at BRW. Discussions with G. Liston, J. King, and G. Wendler were very helpful. T. Zhang, D. Yang, and an anonymous reviewer offered many insightful suggestions. We are appreciative of R. Rosson, who assisted with the formatting of the manuscript.

References

- Aizen, E. M., V. B. Aizen, J. M. Melack, and A. N. Krenke, Heat exchange during snow ablation in plains and mountains of Eurasia, *J. Geophys. Res.*, 105(D22), 27,013–27,022, 2000.
- Aizen, V. B., E. M. Aizen, J. M. Melack, and J. Dozier, Climate and hydrological changes in the Tien Shan, central Asia, *J. Clim.*, 10, 218–229, 1997.
- Beamish, R. J., C. E. Neville, and A. J. Cass, Production of Fraser River sockeye salmon (*Oncorhynchus nerka*) in relation to decadal-scale changes in the climate and the ocean, *Can. J. Fish. Aquat. Sci.*, 54, 543–554, 1997.
- Benson, C. S., Reassessment of winter precipitation on Alaska's Arctic slope and measurement on the flux of wind blown snow, *Rep. 288*, 26 pp., Geophysical Institute, Univ. of Alaska, Fairbanks, 1982.
- Black, R. F., Precipitation at Barrow, Alaska, greater than recorded, *Eos Trans. AGU*, 35(2), 203–206, 1954.
- Bond, N. A., and D. E. Harrison, The Pacific Decadal Oscillation, air-sea interaction, and central North Pacific winter atmospheric regimes, *Geophys. Res. Lett.*, 27(5), 731–734, 2000.
- Brown, R. D., and R. O. Braaten, Spatial and temporal variability of Canadian monthly snow depths, 1946–1995, *Atmos. Ocean*, 36, 37–54, 1998.
- Clagett, P. G., The Wyoming Wind Shield: An evaluation after 12 years of use in Alaska, paper presented at *Western Snow Conference*, Kalispell, Montana, 19–21 April 1988.
- Curry, J. A., J. L. Schramm, and E. E. Ebert, Sea ice-albedo climate feedback mechanism, *J. Clim.*, 8, 240–247, 1995.
- Curtis, J., G. Wendler, R. Stone, and E. Dutton, Precipitation decrease in the western Arctic, with special emphasis on Barrow and Barter Island, Alaska, *Int. J. Climatol.*, 18, 1687–1707, 1998.
- Divoky, G. J., Factors affecting the growth of a Black Guillemot colony in northern Alaska, Ph.D. dissertation, Univ. of Alaska, Fairbanks, 1998.
- Dutton, E. G., and D. J. Endres, Date of snow melt at Barrow, Alaska, USA, *Arct. Alp. Res.*, 23(1), 115–119, 1991.
- Foster, J. L., The significance of the date of snow disappearance on the Arctic tundra as a possible indicator of climatic change, *Arct. Alp. Res.*, 21(1), 60–70, 1989.
- Foster, J. L., J. W. Winchester, and E. G. Dutton, The date of snow disappearance on the Arctic tundra as determined from satellite, meteorological station and radiometric in situ observations, *IEEE Trans. Geosci. Remote Sens.*, 30(4), 793–798, 1992.
- Groisman, P., T. R. Karl, and R. W. Knight, Observed impact of snow cover on the heat balance and the rise of continental spring temperatures, *Science*, 263, 198–200, 1994.
- Harris, J. M., and J. D. W. Kahl, Analysis of 10-day isentropic flow patterns for Barrow, Alaska: 1985–1992, *J. Geophys. Res.*, 99(D12), 25,845–25,855, 1994.

- Houghton, J. T., L. G. M. Filho, B. A. Callander, N. Harris, A. Kattenberg, and K. Maskell (Eds.), *Climate Change 1995: The Science of Climate Change*, 572 pp., Cambridge Univ. Press, New York, 1996.
- Kane, D. L., L. D. Hinzman, J. P. McNamara, Z. Zhang, and C. S. Benson, An overview of a nested watershed study in Arctic Alaska, *Nord. Hydrol.*, *31*, 245–266, 2000.
- Keeling, C. D., J. F. S. Chin, and T. P. Whorf, Increased activity in northern vegetation inferred from atmospheric CO₂ measurements, *Nature*, *382*, 146–149, 1996.
- King, J. C., P. S. Anderson, and G. W. Mann, The seasonal cycle of sublimation at Halley, Antarctica, *J. Glaciol.*, *47*, 1–8, 2001.
- Kuang, Z., and Y. L. Yung, Observed albedo decrease related to the spring snow retreat, *Geophys. Res. Lett.*, *27*(9), 1299–1302, 2000.
- Liston, G. E., and M. Sturm, A snow-transport model for complex terrain, *J. Glaciol.*, *44*(148), 498–516, 1998.
- Maslanik, J. A., M. C. Serreze, and R. G. Barry, Recent decreases in Arctic summer ice cover and linkages to atmospheric circulation anomalies, *Geophys. Res. Lett.*, *23*(13), 1677–1680, 1996.
- Maslanik, J. A., M. C. Serreze, and T. Agnew, On the record reduction in western Arctic sea ice cover in 1998, *Geophys. Res. Lett.*, *26*(13), 1905–1908, 1999.
- Maykut, G. A., and P. E. Church, Radiation climate of Barrow, Alaska, *J. Appl. Meteorol.*, *12*, 620–628, 1973.
- Myneni, R. B., C. D. Keeling, C. J. Tucker, G. Asrar, and R. R. Nemani, Increased plant growth in the northern high latitudes from 1981 to 1991, *Nature*, *386*, 698–702, 1997.
- Natural Resources Conservation Service, Alaska annual data summary, water year 1994, report, U.S. Dep. of Agric., Washington, D. C., 1994.
- Oechel, W. C., G. L. Vourlitis, S. J. Hastings, and S. A. Bochkrez, Effects of Arctic CO₂ flux over two decades: Effects of climate change at Barrow, Alaska, *Ecol. Appl.*, *5*, 846–855, 1995.
- Osterkamp, T. E., and V. E. Romanovsky, Evidence for warming and thawing of discontinuous permafrost in Alaska, *Permafrost Periglacial Proc.*, *5*, 137–144, 1999.
- Overland, J. E., J. M. Adams, and N. A. Bond, Decadal variability of the Aleutian Low and its relation to high-latitude circulation, *J. Clim.*, *12*, 1542–1548, 1998.
- Pomeroy, J. W., P. Marsh, and D. M. Gray, Application of a distributed blowing snow model to the Arctic, *Hydrol. Processes*, *11*, 1451–1464, 1997.
- Ramanathan, V., B. R. Barkstrom, and E. F. Harrison, Climate and the Earth's radiation budget, *Phys. Today*, *42*(5), 22–32, 1989.
- Robinson, D. A., K. F. Dewey, and R. R. Heim, Global snow cover monitoring: An update, *Bull. Am. Meteorol. Soc.*, *74*, 1689–1696, 1993.
- Rothrock, D. A., Y. Yu, and G. A. Maykut, Thinning of the Arctic sea-ice cover, *Geophys. Res. Lett.*, *26*(23), 3469–3472, 1999.
- Serreze, M. C., J. E. Walsh, F. S. Chapin III, T. Osterkamp, M. Dyurgerov, V. Romanovsky, W. C. Oechel, J. Morison, T. Zhang, and R. G. Barry, Observational evidence of recent change in the northern high-latitude environment, *Clim. Change*, *46*, 159–207, 2000.
- Stone, R. S., Variations in western Arctic temperatures in response to cloud-radiative and synoptic-scale influences, *J. Geophys. Res.*, *102*(D18), 21,769–21,776, 1997.
- Stone, R., T. Mefford, E. Dutton, D. Longenecker, B. Halter, and D. Endres, Surface radiation and meteorological measurements: January 1992 to December 1994, *Data Rep. ERL-CMDL-11*, 81 pp., Natl. Oceanic and Atmos. Admin. Environ. Res. Lab., Boulder, Colo., 1996.
- Thompson, D. W. J., and J. M. Wallace, The Arctic Oscillation signature in the wintertime geopotential height and temperature fields, *Geophys. Res. Lett.*, *25*(9), 1297–1300, 1998.
- Thompson, D. W. J., and J. M. Wallace, Annular modes in the extratropical circulation, I, Month-to-month variability, *J. Clim.*, *13*, 1000–1016, 2000.
- Trenberth, K. E., and J. W. Hurrell, Decadal atmosphere-ocean variations in the Pacific, *Clim. Dyn.*, *9*, 303–319, 1994.
- Vinnikov, K. Y., A. Robock, R. J. Stouffer, J. E. Walsh, C. L. Parkinson, D. J. Cavalieri, J. F. B. Mitchell, D. Garrett, and V. F. Zakharov, Global warming and Northern Hemisphere sea ice extent, *Science*, *286*, 1934–1937, 1999.
- Weller, G., and B. Holmgren, The microclimates of the Arctic tundra, *J. Appl. Meteorol.*, *13*, 854–862, 1974.
- Yang, D., B. E. Goodison, C. S. Benson, and S. Ishda, Adjustment of daily precipitation at 10 climate stations in Alaska: Application of the World Meteorological Organization intercomparison results, *Water Resour. Res.*, *34*(2), 241–256, 1998.
- Ye, H., H. Cho, and P. E. Gustafson, The changes of the Russian snow accumulation during 1936–1983 and its spatial patterns, *J. Clim.*, *11*, 856–863, 1998.
- Zhang, T., T. E. Osterkamp, and K. Stamnes, Some characteristics of the climate in northern Alaska, U.S.A., *Arct. Alp. Res.*, *28*(4), 509–518, 1996a.
- Zhang, T., K. Stamnes, and S. A. Bowling, Impact of clouds on surface radiative fluxes and snowmelt in the arctic and subarctic, *J. Clim.*, *9*, 2110–2123, 1996b.
- Zhang, T., T. E. Osterkamp, and K. Stamnes, Effects of climate on the active layer and permafrost on the North Slope of Alaska, U.S.A., *Permafrost Periglacial Proc.*, *8*, 45–67, 1997.
- Zhang, T., T. Haran, and T. Scambos, Spatial and temporal variations of surface albedo and snowmelt in northern Alaska using AVHRR Polar Pathfinder datasets, paper presented at International Geoscience and Remote Sensing Symposium, IEEE Geosci. and Remote Sens. Soc., Honolulu, Hawaii, 24–28 July 2000.
- Zimov, S. A., Y. V. Voropaev, I. P. Semiletov, S. P. Daviudov, S. F. Prosiannikov, F. S. Chapin III, M. C. Chapin, S. Trumbore, and S. Tyler, North Siberian lakes: A methane source fueled by Pleistocene carbon, *Science*, *277*, 800–802, 1997.

E. G. Dutton, J. M. Harris, D. Longenecker, and R. S. Stone, Climate Monitoring and Diagnostics Laboratory, NOAA, 325 Broadway, Boulder, CO 80305, USA. (edutton@cmdl.noaa.gov; jharris@cmdl.noaa.gov; dlongenecker@cmdl.noaa.gov; Robert.Stone@noaa.gov)

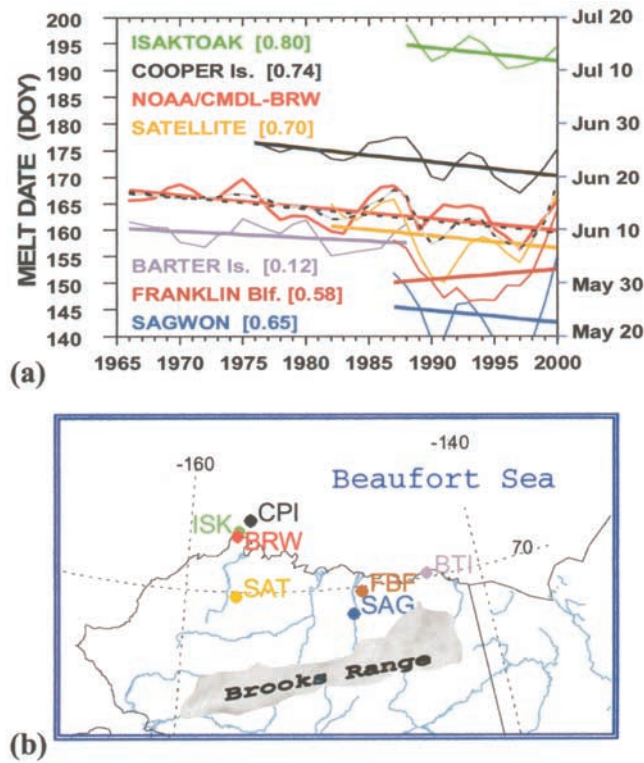


Figure 3. Analyses of six independent time series of melt dates compared with the 1966–2000 BRW record (from Figure 2). The 5-year smoothed time series and linear fits are shown. Each is correlated with the NOAA/CMDL-BRW record with coefficients indicated for each of the sites described in the text. The dashed-curve analysis (unlabeled) is for an ensemble average of the 142 station-years, normalized to the BRW timeframe. (b) Map of Alaska’s North Slope showing the location of sites making up the ensemble. Details of data and site descriptions are given in the text.